

# Approximation Algorithm for Noisy Quantum Circuit Simulation

1<sup>st</sup> Mingyu Huang

*Institute of Software, Chinese Academy of Sciences*  
*University of Chinese Academy of Sciences*  
Beijing, China  
huangmy@ios.ac.cn

2<sup>nd</sup> Ji Guan

*Institute of Software, Chinese Academy of Sciences*  
Beijing, China  
guanji@ios.ac.cn

3<sup>rd</sup> Wang Fang

*Institute of Software, Chinese Academy of Sciences*  
*University of Chinese Academy of Sciences*  
Beijing, China  
fangw@ios.ac.cn

4<sup>th</sup> Mingsheng Ying

*Institute of Software, Chinese Academy of Sciences*  
*Tsinghua University*  
Beijing, China  
yingms@ios.ac.cn

**Abstract**—Simulating noisy quantum circuits is vital in designing and verifying quantum algorithms in the current NISQ (Noisy Intermediate-Scale Quantum) era, where quantum noise is unavoidable. However, it is much more inefficient than the classical counterpart because of the quantum state explosion problem (the dimension of state space is exponential in the number of qubits) and the complex (non-unitary) representation of noises. Consequently, only noisy circuits with up to about 50 qubits can be simulated approximately well. This paper introduces a novel approximation algorithm for simulating noisy quantum circuits when the noisy effectiveness is insignificant to improve the scalability of the circuits that can be simulated. The algorithm is based on a new tensor network diagram for the noisy simulation and uses the singular value decomposition to approximate the tensors of quantum noises in the diagram. The contraction of the tensor network diagram is implemented on Google’s TensorNetwork. The effectiveness and utility of the algorithm are demonstrated by experimenting on a series of practical quantum circuits with realistic superconducting noise models. As a result, our algorithm can approximately simulate quantum circuits with up to 225 qubits and 20 noises (within about 1.8 hours). In particular, our method offers a speedup over the commonly-used approximation (sampling) algorithm — quantum trajectories method [1]. Furthermore, our approach can significantly reduce the number of samples in the quantum trajectories method when the noise rate is small enough.

**Index Terms**—Quantum circuits, noisy simulation, approximation algorithm, tensor network

## I. INTRODUCTION

Since the achievement of quantum supremacy over classical computing [2], quantum processors with an increasing number of quantum bits (qubits) [3], [4] have been manufactured. This progress has marked the transition to the NISQ (Noisy Intermediate-Scale Quantum) era [5]. Even though current quantum processors have a limited number of qubits and are susceptible to quantum noise, they’ve been used in numerous applications, highlighting the potential benefits of NISQ devices [6]–[8]. The circuits that carry out computational tasks are at the heart of these processors.

Building and testing quantum circuits in real-world environments is crucial in quantum computing. These environments often introduce *noises*, a common challenge in the NISQ era. Simulating these circuits on classical computers before building them is beneficial—it saves costs and helps avoid potential issues when implementing quantum circuits and reading outputs from real devices. Consequently, it is urgently necessary to develop efficient simulation algorithms for noisy quantum circuits.

**Noiseless Simulation:** The widely used method of noiseless simulation is to calculate the transitions of the state vector through a sequence of quantum gates modeled by unitary matrices. This method is straightforward and integrated into most popular software development kits for quantum computing (e.g., Qiskit, Cirq, etc.). However, the exponential number of terms in these representations restricts the number of qubits that can be simulated. To overcome this issue, one popular method employs a data structure, the *tensor network*, to capture the locality (a quantum gate is only applied on 1 or 2 qubits) and regularity (the pattern of quantum gates in practical circuits is regular) of quantum circuits. This approach has been successfully utilized in simulating large noiseless quantum circuits [9]–[14]. An alternative approach is the Decision Diagram-based (DD-based) method [15], [16], akin to the Binary Decision Diagrams (BDD) in classical computing. This technique optimizes memory usage and performance by compactly storing all state amplitudes in a specialized data structure. While effective for certain types of circuits, particularly those that maintain manageable data structure sizes throughout the simulation, its performance diminishes with circuits that have gates with arbitrary parameters, such as those used in quantum supremacy experiments [15], [17].

**Noisy Simulation:** For simulating noisy quantum circuits, most software packages [18], [19] employ the density matrix representation. While this approach is standard, it struggles with scalability when applied to circuits with a high qubit

count. To enhance the scalability of noisy circuit simulations, several approximation algorithms have been introduced. These include the quantum trajectories method, which offers a probabilistic approach to simulate noise effects [1]. Algorithms such as MPS (Matrix Product State) [20], MPO (Matrix Product Operators) [21], [22], and MPDO (Matrix Product Density Operators) [23] use tensor network representations along with SVD (singular value decomposition) for approximation. The DD-based simulation can also be extended to noisy simulation for some specific circuits and noise types [24]. However, challenges like the quantum state explosion problem restrict current simulations to about 50 qubits. The simulation demand of the NISQ circuits with up to hundreds of qubits cannot be satisfied.

**Contributions of This Paper:** To address this gap, we developed a new approximation algorithm for simulating noisy quantum circuits. We introduce a novel tensor network diagram for this simulation. In our diagram, noisy quantum circuits are represented by double-size tensors and can be well approximated by performing SVD on their tensor representation. Based on these, an approximation algorithm is developed and implemented with Google TensorNetwork [25]. The effectiveness and utility of our algorithm are confirmed by experimenting with three types of practical quantum circuits (algorithms). The experimental results show that our algorithm can approximately simulate quantum circuits with up to 225 qubits and 20 noises (within about 1.8 hours). In particular, our method offers a speedup over the commonly-used approximation (sampling) algorithm — quantum trajectories method [1].

## II. PRELIMINARY

**Basics of Quantum Computation:** We start by recalling some basic concepts of quantum circuits. Ideally, a quantum computer without noise is a closed system. In this case, quantum data are mathematically modeled as complex unit vectors in a  $2^n$ -dimensional Hilbert (linear) space  $\mathcal{H}$ . Such a quantum datum is usually called a *pure state* and written as  $|\psi\rangle$  in the Dirac notation, and  $n$  represents the number of involved *quantum bits (qubits)*. Specifically, a qubit is a quantum datum in a 2-dimensional Hilbert space, denoted by  $|q\rangle = \begin{pmatrix} a \\ b \end{pmatrix} = a|0\rangle + b|1\rangle$  with  $|0\rangle = \begin{pmatrix} 1 \\ 0 \end{pmatrix}$  and  $|1\rangle = \begin{pmatrix} 0 \\ 1 \end{pmatrix}$ , where complex numbers  $a$  and  $b$  satisfy the normalization condition  $|a|^2 + |b|^2 = 1$ . Here, the orthonormal basis  $\{|0\rangle, |1\rangle\}$  of the Hilbert space corresponds to the values  $\{0, 1\}$  of a bit in classical computers. A quantum computing task is implemented by a *quantum circuit*, which is mathematically represented by a  $2^n \times 2^n$  unitary matrix  $U$ , i.e.,  $U^\dagger U = U U^\dagger = I_n$ , where  $U^\dagger$  is the (entry-wise) conjugate transpose of  $U$  and  $I_n$  is the identity matrix on  $\mathcal{H}$ . For an input  $n$ -qubit datum  $|\psi\rangle$ , the output of the circuit is a datum of the same size:  $|\psi'\rangle = U|\psi\rangle$ .

Like its classical counterpart, a quantum circuit  $U$  consists of a sequence (product) of *quantum logic gates*  $U_i$ , i.e.,  $U = U_d \cdots U_1$ . Here  $d$  is the gate number of the circuit  $U$ . Each gate  $U_i$  only non-trivially operates on one or two qubits. We

TABLE I: 1-QUBIT GATE

H	$\frac{1}{\sqrt{2}} \begin{pmatrix} 1 & 1 \\ 1 & -1 \end{pmatrix}$	X ( $\sigma_x$ )	$\begin{pmatrix} 0 & 1 \\ 1 & 0 \end{pmatrix}$
Y ( $\sigma_y$ )	$\begin{pmatrix} 0 & -i \\ i & 0 \end{pmatrix}$	Z ( $\sigma_z$ )	$\begin{pmatrix} 1 & 0 \\ 0 & -1 \end{pmatrix}$
T	$\begin{pmatrix} 1 & 0 \\ 0 & e^{i\pi/4} \end{pmatrix}$	$R_x(\theta)$	$\begin{pmatrix} \cos \frac{\theta}{2} & -i \sin \frac{\theta}{2} \\ -i \sin \frac{\theta}{2} & \cos \frac{\theta}{2} \end{pmatrix}$
$R_y(\theta)$	$\begin{pmatrix} \cos \frac{\theta}{2} & -\sin \frac{\theta}{2} \\ \sin \frac{\theta}{2} & \cos \frac{\theta}{2} \end{pmatrix}$	$R_z(\theta)$	$\begin{pmatrix} e^{-i\theta/2} & 0 \\ 0 & e^{i\theta/2} \end{pmatrix}$

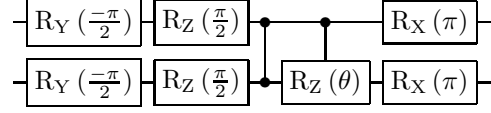


Fig. 1: A 2-qubit QAOA circuit

list commonly used 1-qubit gates in Table I. Arbitrary 1-qubit gates can be decomposed into 1-qubit rotation gates  $R_x(\theta)$ ,  $R_y(\theta)$  and  $R_z(\theta)$  with rotation parameter  $\theta$ . In addition, for any 1-qubit logic gate  $U$ , we can generate a 2-qubit logic gate — controlled- $U$  (CU) gate, applying  $U$  on the second (target) qubit if and only if the first (control) qubit is  $|1\rangle$ . Specifically, the controlled-Z (CZ) gate (commonly used in superconducting quantum circuits) and the general controlled- $U$  gate are illustrated as follows. Fig. 1 shows an example of a 2-qubit quantum circuit for the QAOA algorithm.

$$\begin{array}{c} \text{---} \\ \bullet \\ \text{---} \\ \boxed{U} \\ \text{---} \end{array} = \begin{pmatrix} 1 & 0 & 0 & 0 \\ 0 & 1 & 0 & 0 \\ 0 & 0 & u_{00} & u_{01} \\ 0 & 0 & u_{10} & u_{11} \end{pmatrix} \quad \begin{array}{c} \text{---} \\ \text{---} \\ \bullet \\ \bullet \\ \text{---} \end{array} = \begin{pmatrix} 1 & 0 & 0 & 0 \\ 0 & 1 & 0 & 0 \\ 0 & 0 & 1 & 0 \\ 0 & 0 & 0 & -1 \end{pmatrix}$$

**Quantum Noises:** In the current NISQ era, quantum noise is unavoidable, so we have to consider the noisy effect in quantum computing. Consequently, the uncertainty will be brought such that quantum states become mixed instead of pure states. A *mixed state* is considered as an ensemble  $\{(p_k, |\psi_k\rangle)\}$ , meaning the quantum system is in state  $|\psi_k\rangle$  with probability  $p_k$ . Mathematically, it can be described by a  $2^n \times 2^n$  *density matrix*  $\rho$  (Hermitian positive semidefinite matrix with unit trace<sup>1</sup>) on  $\mathcal{H}$ :  $\rho = \sum_k p_k |\psi_k\rangle \langle \psi_k|$ , where  $\langle \psi_k|$  is the conjugate transpose of  $|\psi_k\rangle$ , i.e.,  $\langle \psi_k| = |\psi_k\rangle^\dagger$ . In this situation, a computational task starting at a mixed state  $\rho$  is finished by a mapping  $\mathcal{E}$ :  $\rho' = \mathcal{E}(\rho)$ , where  $\mathcal{E}$  is a quantum channel. A channel  $\mathcal{E}$  (also called a *super-operator*) admits a *Kraus matrix form* [26]: there exists a finite set  $\{E_k\}_{k \in \mathcal{K}}$  of matrices on  $\mathcal{H}$  such that

$$\mathcal{E}(\rho) = \sum_{k \in \mathcal{K}} E_k \rho E_k^\dagger \quad \text{with} \quad \sum_{k \in \mathcal{K}} E_k^\dagger E_k = I_n,$$

where  $\{E_k\}_{k \in \mathcal{K}}$  is called *Kraus matrices* of  $\mathcal{E}$ . Specifically, quantum gate  $U$  can be viewed as a unitary channel where  $\mathcal{E}(\rho) = U \rho U^\dagger$ . Briefly,  $\mathcal{E}$  is represented as  $\mathcal{E} = \{E_k\}_{k \in \mathcal{K}}$ . Quantum noises can be represented as quantum channels. An

<sup>1</sup> $\rho$  has unit trace if  $\text{tr}(\rho) = 1$ , where trace  $\text{tr}(\rho)$  of  $\rho$  is defined as the summation of diagonal elements of  $\rho$ .

example of quantum noise is the depolarizing noise, which is represented as  $\{\sqrt{1-p}I, \sqrt{\frac{p}{3}}X, \sqrt{\frac{p}{3}}Y, \sqrt{\frac{p}{3}}Z\}$ . Similar to noiseless quantum circuit  $U$ , noisy quantum circuit  $\mathcal{E}$  also consists of a sequence (mapping composition) of (noisy) gates  $\{\mathcal{E}_i\}$ , i.e.,  $\mathcal{E} = \mathcal{E}_d \circ \dots \circ \mathcal{E}_1$ , where each  $\mathcal{E}_i$  is either a noiseless gate or a noise channel.

The only way allowed by quantum mechanics to extract classical information is through a quantum measurement, which is mathematically modeled by a set  $\{P_i\}_{i \in \mathcal{O}}$  of projection matrices on its state (Hilbert) space  $\mathcal{H}$  with  $\mathcal{O}$  being the set of outputs and  $\sum_{i \in \mathcal{O}} P_i = I_n$ . This observing process is probabilistic: for a given quantum state  $\rho$ , a measurement outcome  $i \in \mathcal{O}$  is obtained with probability  $p_i = \text{tr}(P_i \rho)$ .

### III. NOISY QUANTUM CIRCUIT SIMULATION

The simulation task for noiseless quantum circuit is to calculate the state vector representation of the output state of a circuit for a given input state. For noisy quantum circuits, the simulation task targets to estimate the density matrix of the output state. Specifically, given a noisy quantum circuit  $\mathcal{E}_{\mathcal{N}}$  and input state  $\rho_0$ , the goal of the noisy simulation task is to estimate  $\mathcal{E}_{\mathcal{N}}(\rho_0)$ . Every element of  $\mathcal{E}_{\mathcal{N}}(\rho_0)$  can be independently estimated by  $\langle x | \mathcal{E}_{\mathcal{N}}(\rho_0) | y \rangle$ , where  $|x\rangle, |y\rangle$  are pure states ranging from all computational basis of  $\mathcal{H}$ . Furthermore, we observe that the value of  $\langle x | \mathcal{E}_{\mathcal{N}}(\rho_0) | y \rangle$  can be computed by the following way:

$$\begin{aligned} \langle x | \mathcal{E}_{\mathcal{N}}(\rho_0) | y \rangle &= \frac{1}{4} (\langle (x| + \langle y|) | \mathcal{E}_{\mathcal{N}}(\rho_0) (|x\rangle + |y\rangle) \\ &\quad - \langle (x| - \langle y|) | \mathcal{E}_{\mathcal{N}}(\rho_0) (|x\rangle - |y\rangle) \\ &\quad - i \langle (x| - i \langle y|) | \mathcal{E}_{\mathcal{N}}(\rho_0) (|x\rangle + i |y\rangle) \\ &\quad + i \langle (x| + i \langle y|) | \mathcal{E}_{\mathcal{N}}(\rho_0) (|x\rangle - i |y\rangle) \end{aligned}$$

Therefore the key to simulating a noisy quantum circuit is as follows.

**Problem 1** (Noisy Simulation Task of Quantum Circuits). *Given a noisy quantum circuit with  $d$  gates  $\mathcal{E}_{\mathcal{N}} = \mathcal{E}_d \circ \dots \circ \mathcal{E}_1$  [26], an input state  $|\psi\rangle$  and a state  $|v\rangle$ , the noisy simulation of quantum circuit  $\mathcal{E}_{\mathcal{N}}$  on  $|\psi\rangle$  is to estimate  $\langle v | \mathcal{E}_{\mathcal{N}}(|\psi\rangle\langle\psi|) | v \rangle$  (with a high accuracy).*

This paper aims to solve the problem using tensor networks as the data structure for modeling quantum circuits and SVD for approximating the tensor representation of quantum noise. Tensor networks provide a graphical representation for quantum systems and their interactions. The tensor diagrams offer an intuitive way to understand and process the behavior of quantum circuits (see [27] for more details). In the following, we introduce a tensor network diagram for the noisy simulation task in Problem 1, which is the foundation for our approximation simulation algorithm. Furthermore, this diagram directly leads to a tensor network-based algorithm for exactly computing  $\langle v | \mathcal{E}_{\mathcal{N}}(|\psi\rangle\langle\psi|) | v \rangle$ .

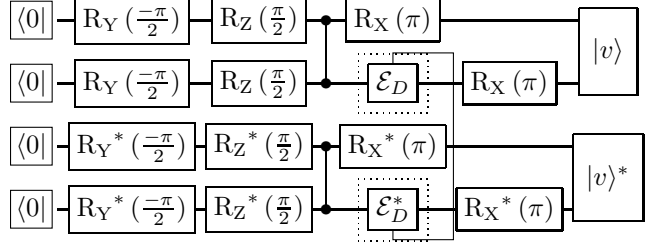


Fig. 2: Tensor network diagram of the 2-qubit QAOA circuit in Fig. 1 with input state  $|0\rangle$ .

**Tensor Network Diagram for Noisy Simulation:** To compute  $\langle v | \mathcal{E}_{\mathcal{N}}(|\psi\rangle\langle\psi|) | v \rangle$ , one can utilize the matrix representation of quantum super-operators [28, Chapter 2.2.2].

$$\begin{aligned} \langle v | \mathcal{E}_{\mathcal{N}}(|\psi\rangle\langle\psi|) | v \rangle &= \text{tr}(|v\rangle\langle v| \mathcal{E}_{\mathcal{N}}(|\psi\rangle\langle\psi|)) \\ &= \langle \Omega | [ |v^*\rangle\langle v^*| \otimes \mathcal{E}_{\mathcal{N}}(|\psi\rangle\langle\psi|) ] | \Omega \rangle \\ &= \langle \Omega | [ |v^*\rangle\langle v^*| \otimes \mathcal{E}_d \circ \dots \circ \mathcal{E}_1(|\psi\rangle\langle\psi|) ] | \Omega \rangle \\ &= \langle v | \otimes \langle v^* | (M_{\mathcal{E}_d} \dots M_{\mathcal{E}_1}) | \psi \rangle \otimes | \psi^* \rangle \end{aligned}$$

where  $|\psi^*\rangle$  is the entry-wise conjugate of  $|\psi\rangle$ ,  $|\Omega\rangle$  is the (unnormalized) maximal entangled state, i.e.,  $|\Omega\rangle = \sum_j |j\rangle \otimes |j\rangle$  with  $\{|j\rangle\}$  being an orthonormal basis of Hilbert space  $\mathcal{H}$ , and  $M_{\mathcal{E}} = \sum_k E_k \otimes E_k^*$  is called the *matrix representation* of  $\mathcal{E}$ , where  $\mathcal{E}(\rho) = \sum_k E_k \rho E_k^\dagger$  with Kraus operators  $\{E_k\}_{k \in \mathcal{K}}$ . The tensor diagram can visualize this representation.

We note that  $M_{\mathcal{E}} = \sum_{k \in \mathcal{K}} E_k \otimes E_k^*$  represents the noises in the newly obtained tensor network. In particular, for a unitary super-operator  $\mathcal{U}(\rho) = U \rho U^\dagger$  with unitary operator  $U$ ,  $M_{\mathcal{U}}$  is depicted as the right tensor network in the following.

$$M_{\mathcal{E}} = \sum_{k \in \mathcal{K}} E_k \otimes E_k^* = \begin{array}{c} \boxed{E_k} \\ \boxed{E_k^*} \end{array} \quad M_{\mathcal{U}} = U \otimes U^* = \begin{array}{c} \boxed{U} \\ \boxed{U^*} \end{array}$$

Based on these observations, we get a serial connection of the two tensor networks representing  $n$ -qubit circuits  $\mathcal{E}_{\mathcal{N}}$ . Subsequently, we derived an accuracy algorithm to compute  $\langle v | \otimes \langle v^* | (M_{\mathcal{E}_d} \dots M_{\mathcal{E}_1}) | \psi \rangle \otimes | \psi^* \rangle$  by contracting a tensor network with double size ( $2n$  qubits). An illustration of the tensor network diagram of the two-qubit noisy QAOA circuit of Fig. 1 is shown in Fig. 2.

### IV. APPROXIMATION ALGORITHM FOR NOISY QUANTUM CIRCUIT SIMULATION

We are ready to present our approximation noisy simulation algorithm based on the new tensor network diagram.

**Approximation Noisy Simulation Algorithm:** As we can see, the noises make simulating a quantum circuit much harder. To handle the difficulty of simulating a circuit with a large number of noises, we introduce an approximation noisy circuit simulation method based on the matrix representation and the SVD (Singular Value Decomposition), which can balance the accuracy and efficiency of the simulation. The insight of our

method starts with an observation that most noises occurring in physical quantum circuits are close to the identity operators (matrices). Take the depolarizing noise as an example, which is defined by

$$\mathcal{E}(\rho) = (1-p)\rho + \frac{p}{3}(X\rho X + Y\rho Y + Z\rho Z).$$

Probability  $p$  can be regarded as a metric of the noisy effectiveness of the channel. When  $p$  is small, the noise is almost identical to the identity channel. Therefore, a straightforward method is to approximately represent the depolarizing channel by  $(1-p)I$ . The current physical implementation of practical quantum algorithms requires that the effectiveness of noise is insignificant. For general noise  $\mathcal{E}$ , we define  $\|M_{\mathcal{E}} - I\|$  as the *noise rate* of  $\mathcal{E}$ , where  $\|\cdot\|$  is the 2-norm of matrix. For example, the depolarizing noise with parameter  $p$  has a noise rate  $2p$ . Next, we will describe our approximation algorithm and explain why it is efficient when the noise rate is small.

To handle the noises, we perform SVD on the matrix representation of each noise as illustrated in Fig. 3.

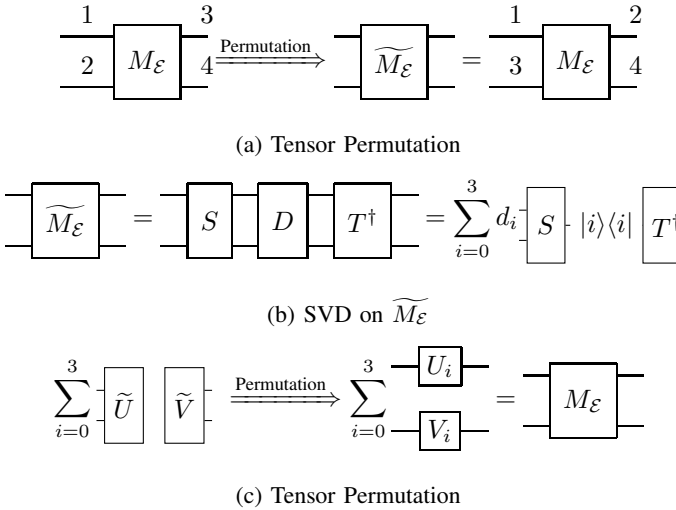


Fig. 3: Decomposition of  $M_{\mathcal{E}}$

Suppose we treat  $M_{\mathcal{E}}$  as a tensor with rank 4, and the edges are indexed as in Fig. 3 (a).  $M_{\mathcal{E}}$  is the matrix with edges 1, 2 being the row and 3, 4 being the column. We introduce the tensor permutation operator where  $\tilde{M}_{\mathcal{E}}$  is the matrix with 1, 3 being the row and 2, 4 being the column. For example, the identity operator  $I$  on two qubits and its tensor permutation  $\tilde{I}$  are:

$$I = \begin{pmatrix} 1 & 0 & 0 & 0 \\ 0 & 1 & 0 & 0 \\ 0 & 0 & 1 & 0 \\ 0 & 0 & 0 & 1 \end{pmatrix} \quad \tilde{I} = \begin{pmatrix} 1 & 0 & 0 & 1 \\ 0 & 0 & 0 & 0 \\ 0 & 0 & 0 & 0 \\ 1 & 0 & 0 & 1 \end{pmatrix}$$

Performing SVD on  $\tilde{M}_{\mathcal{E}}$  we have  $\tilde{M}_{\mathcal{E}} = SDT^\dagger$ , where  $D = \sum_{i=0}^3 d_i |i\rangle\langle i|$  and  $d_0$  is the most significant singular value (see Fig. 3(b)). Let  $\tilde{U}_i = d_i S |i\rangle$  and  $\tilde{V}_i = T |i\rangle$  as in the left of Fig. 3 (c), we get  $\tilde{M}_{\mathcal{E}} = \sum_{i=0}^3 \tilde{U}_i \tilde{V}_i^\dagger$ . Then use tensor

permutation again on  $\tilde{U}_i$  and  $\tilde{V}_i$  (here  $\tilde{U}_i$  is treated as a rank 4 tensor with index 3,4 being 0-dimension, and  $\tilde{V}_i$  is treated as a rank 4 tensor with index 1,2 being 0-dimension), we get  $M_{\mathcal{E}} = \sum_{i=0,1,2,3} U_i \otimes V_i$ , as illustrated in Fig. 3 (c).

Next, we will show that when the noise rate of  $\mathcal{E}$  is small,  $U_0 \otimes V_0$  is a good approximation of  $M_{\mathcal{E}}$ .

**Lemma 1.** *Suppose  $A$  and  $B$  are all  $4 \times 4$  matrices, and  $\tilde{A}$  and  $\tilde{B}$  are the tensor permutation of  $A$  and  $B$  as defined before. If  $\|A - B\| < \delta$ , then we have  $\|\tilde{A} - \tilde{B}\| < 2\delta$ .*

*Proof.* We use  $\|\cdot\|_F$  to denote the Frobenius norm of matrices. Specifically, for  $4 \times 4$  matrices, it can be shown that  $\|A\| \leq \|A\|_F \leq 2\|A\|$ . Note that  $A$  and  $\tilde{A}$  have the same Frobenius norm since the tensor permutation operator only rearranges the positions of elements. Therefore we have  $\|\tilde{A} - \tilde{B}\| \leq \|\tilde{A} - \tilde{B}\|_F = \|A - B\|_F \leq 2\|A - B\| < 2\delta$ .  $\square$

**Lemma 2.** *Suppose  $\|M_{\mathcal{E}} - I\| < \delta$ , then we have  $\|M_{\mathcal{E}} - U_0 \otimes V_0\| < 4\delta$*

*Proof.* By Lemma 1. we have  $\|\tilde{M}_{\mathcal{E}} - \tilde{I}\| < 2\delta$ . Suppose we perform SVD on  $\tilde{M}_{\mathcal{E}}$  we have  $\tilde{M}_{\mathcal{E}} = SDT^\dagger$ . And let  $D_0 = d_0 |0\rangle\langle 0|$ , we have

$$\|\tilde{M}_{\mathcal{E}} - SD_0 T^\dagger\| = \min_{\text{rank}(A)=1} \|\tilde{M}_{\mathcal{E}} - A\| \leq \|\tilde{M}_{\mathcal{E}} - \tilde{I}\| < 2\delta.$$

The first equation comes from the Eckart-Young-Mirsky theorem [29]. The last inequality holds because  $\tilde{I}$  has rank 1. And note that  $\tilde{M}_{\mathcal{E}} = M_{\mathcal{E}}$  and  $\tilde{SD_0 T^\dagger} = U_0 \otimes V_0$ , by Lemma 1, we have

$$\|M_{\mathcal{E}} - U_0 \otimes V_0\| < 4\delta. \quad \square$$

We are ready to introduce our approximation algorithm for the noisy quantum circuit simulation task. Suppose  $\mathcal{E}_{\mathcal{N}} = \mathcal{E}_d \circ \dots \circ \mathcal{E}_1$  is a quantum circuit with  $N$  noises, where the noise channels have index  $\{i_1, \dots, i_N\}$ . After applying SVD on each matrix representation of noises we get  $M_{\mathcal{E}_{i_s}} = U_0^s \otimes V_0^s + U_1^s \otimes V_1^s + U_2^s \otimes V_2^s + U_3^s \otimes V_3^s$ ,  $s \in \{1, \dots, N\}$ , where  $M_{\mathcal{E}_{i_s}}$  is closed to  $U_0^s \otimes V_0^s$ . The idea of our algorithm is to calculate the simulation result by using  $U_0^s \otimes V_0^s$  to substitute the noises as a prior choice. Let  $M'_{\mathcal{E}_{i_s}} = U_0^s \otimes V_0^s$  and  $\overline{M_{\mathcal{E}_{i_s}}} = U_1^s \otimes V_1^s + U_2^s \otimes V_2^s + U_3^s \otimes V_3^s$ . Thus  $M_{\mathcal{E}_{i_s}} = M'_{\mathcal{E}_{i_s}} + \overline{M_{\mathcal{E}_{i_s}}}$  and  $\|\overline{M_{\mathcal{E}_{i_s}}}\| < 4p$  by Lemma 2. Let  $T_u$  be the sum of tensor networks obtained by substituting all but  $u$  noises to  $M'_{\mathcal{E}_{i_s}}$  and  $u$  noises to one of  $U_i^s \otimes V_i^s$ ,  $i = 1, 2, 3$ ,

i.e.,  $T_u = \sum_{1 \leq p_1 < \dots < p_u \leq N} \prod_{r=1}^u \overline{M_{\mathcal{E}_{i_{p_r}}}} \prod_{t \notin \{p_1, \dots, p_u\}} M'_{\mathcal{E}_{i_t}}$ . We call

$A(l) = \sum_{u=0}^l T_u$  the  $l$ -level approximation of  $\mathcal{E}_{\mathcal{N}}$ . By increasing the approximation level  $l$  we get a better approximation for  $\mathcal{E}_{\mathcal{N}}$ , when  $l = N$ ,  $A(l) = M_{\mathcal{E}_{\mathcal{N}}}$  exactly. Our algorithm is to calculate  $A(l)$  for a given  $l$ . Details of the algorithm are shown in Algorithm 1.

**Theorem 1.** *Given a noisy quantum circuits  $\mathcal{E}_{\mathcal{N}}$  with  $d$  gates and  $N$  noises with all noise rates being less than  $p$ , i.e.,  $\|M_{\mathcal{E}_{i_s}} - I\| < p$  for  $s \in \{1, \dots, N\}$ ,  $i_s \in \{1, \dots, d\}$ . For*

---

**Algorithm 1** ApproximationNoisySimulation( $\mathcal{E}_N, |\psi\rangle, |v\rangle, l$ )

---

**Input:** A noisy quantum circuit  $\mathcal{E}_N = \mathcal{E}_d \circ \dots \circ \mathcal{E}_1$  with  $N$  noises, where the noise channels have index  $\{i_1, \dots, i_N\}$  and Kraus matrices  $\mathcal{E}_{i_s} = \{E_{sk}\}_{k \in \mathcal{K}_s}$  for  $1 \leq s \leq N$ , a test state  $|\psi\rangle$ , an expected output  $|v\rangle$  and a level for the approximation  $l$ .

**Output:**  $A(l)$ , the  $l$ -level approximation of  $\langle v | \mathcal{E}_N(|\psi\rangle\langle\psi|) |v\rangle$

- 1: Result = 0
  - 2: Generate the tensor network as in the accuracy algorithm.
  - 3: Perform tensor permutation and SVD operation to the matrix representation of all noises  $M_{\mathcal{E}_{i_s}}$ , obtaining  $U_k^s$  and  $V_k^s$ , where  $M_{\mathcal{E}_{i_s}} = U_0^s \otimes V_0^s + U_1^s \otimes V_1^s + U_2^s \otimes V_2^s + U_3^s \otimes V_3^s$ ,  $s \in \{1, \dots, N\}$ .
  - 4: **for each**  $0 \leq k \leq l$  **do**
  - 5:     Calculate approximation of level  $k$ :
  - 6:      $T_k := 0$
  - 7:     **for each**  $1 \leq p_1 < \dots < p_k \leq N$  **do**
  - 8:         Substitute  $M_{\mathcal{E}_{i_{p_j}}}$  with one of  $U_1^{p_j} \otimes V_1^{p_j}, U_2^{p_j} \otimes V_2^{p_j}, U_3^{p_j} \otimes V_3^{p_j}$  for  $j \in \{1, \dots, k\}$ . For  $s \notin \{p_1, p_2, \dots, p_k\}$ , substitute  $M_{\mathcal{E}_{i_s}}$  to  $U_0^s \otimes V_0^s$ .
  - 9:     After substitution, the original (double-sized) tensor network is split into two tensor networks, contract both tensor networks, and multiply the result, donated as  $X$ .
  - 10:      $T_k += X$ .
  - 11:     **end for**
  - 12:     Result +=  $T_k$ .
  - 13: **end for**
  - 14: **return** Result
- 

any input and output state  $|\psi\rangle$  and  $|v\rangle$ , donate the fidelity as  $F = \langle v | \mathcal{E}_N(|\psi\rangle\langle\psi|) |v\rangle$ , we have  $|F - A(l)| < (1 + 8p)^N - \sum_{i=0}^l \binom{N}{i} (4p)^i (1 + 4p)^{(N-i)}$ , and the number of tensor network contractions is  $2 \sum_{i=0}^l \binom{N}{i} 3^i$ .

*Proof.*

$$\begin{aligned} |F - A(l)| &= \|M_{\mathcal{E}_N} \cdots M_{\mathcal{E}_1} - \sum_{i=0}^l T_i\| \\ &= \left\| \sum_{i=l+1}^N T_i \right\| \\ &\leq \sum_{i=l+1}^N \|T_i\| \\ &\leq \sum_{i=l+1}^N \binom{N}{i} (4p)^i (1 + 4p)^{(N-i)} \\ &= (1 + 8p)^N - \sum_{i=0}^l \binom{N}{i} (4p)^i (1 + 4p)^{(N-i)} \end{aligned}$$

Therefore

$$\begin{aligned} &\langle v | \otimes \langle v^* | (M_{\mathcal{E}_N} - M'_{\mathcal{E}_N}) |\psi\rangle \otimes |\psi^*\rangle \\ &\leq \| |v\rangle \otimes \langle v^* | \| \| (M_{\mathcal{E}_N} - M'_{\mathcal{E}_N}) |\psi\rangle \otimes |\psi^*\rangle \| \leq \|M_{\mathcal{E}_N} - M'_{\mathcal{E}_N}\| \\ &= (1 + 8p)^N - \sum_{i=0}^l \binom{N}{i} (4p)^i (1 + 4p)^{(N-i)} \quad \square \end{aligned}$$

Specifically, when using the one-level approximation where the number of noises is  $N$  and the noise rate is  $p$ , Theorem 1

asserts that our method has accuracy  $(1 + 8p)^N - 1 - 4Np(1 + 4p)^{N-1}$ . With the assumption that  $p \leq \frac{1}{8N}$ , we have

$$\begin{aligned} &(1 + 8p)^N - 1 - 4Np(1 + 4p)^{N-1} \\ &= \sum_{k=2}^N \binom{N}{k} (4p)^k (1 + 4p)^{N-k} \\ &\leq \left(1 + \frac{1}{2N}\right)^N \sum_{k=2}^N (4Np)^k \\ &\leq \sqrt{e} (4Np)^2 \frac{1 - (4Np)^{N-1}}{1 - 4Np} \\ &\leq 32\sqrt{e} N^2 p^2 \end{aligned}$$

As a comparison, the quantum trajectories method [1] needs  $r$  samples (tensor network contraction) to obtain a result within accuracy  $O(1/\sqrt{r})$  under a constant possibility. For the quantum trajectories method to achieve such accuracy (under a constant probability),  $N^2 p^2 = \frac{C}{\sqrt{r}}$ . Therefore the sample number  $r = \frac{C^2}{N^4 p^4}$ , where  $C$  is a constant number. Note that our level-1 approximation needs  $O(N)$  samples, and therefore our approximation method will need less sampling number than the Monte-Carlo method when  $p = O(N^{-\frac{3}{2}})$ .

## V. EXPERIMENTS

In this section, we demonstrate the utility and effectiveness of our approximation algorithm by simulating various quantum circuits with realistic noise models. In particular, we compare our algorithm with state-of-the-art accurate and approximate methods for the same task, and further numerically analyze our algorithm in terms of accuracy, approximation levels, and noise rate. The code of our implementation can be accessed at Github repository <sup>2</sup>.

**Runtime Environment:** All our experiments are carried out on a server with Intel Xeon Platinum 8153 @ 2.00GHz  $\times$  256 Cores, 2048 GB Memory. The machine runs CentOS 7.7.1908. We use the Google TensorNetwork Python package [25] for the tensor network computation.

**Benchmark Circuits and Fault Models:** Our benchmark circuits consist of three types of quantum circuits: Quantum Approximate Optimization Algorithm (QAOA), Hartree-Fock Variational Quantum Eigensolver (VQE), and random quantum circuits exhibiting quantum supremacy from Google. Google has experimentally run all three types of quantum circuits on their quantum processors. In our experiments, the benchmark circuits are taken from ReCirq [30], an open-source library for Cirq and Google's Quantum Computing Service. The QAOA and VQE circuits are named *qaoa\_N* and *hf\_N* respectively, where  $N$  denotes the number of qubits. The random quantum supremacy circuits with  $R \times C$  qubits and depth  $D$  are named *inst\_R  $\times$  C\_D*.

We use a realistic decoherence noise model of superconducting quantum circuits to model faults [31]. Each decoherence noise is appended after a randomly chosen gate in the circuit.

<sup>2</sup><https://github.com/Veri-Q/VeriQSim>

This emulates the types of errors seen on actual quantum hardware.

The benchmarks and noise models provide a real-world testbed for our techniques. By evaluating our approximation algorithm on these practical circuits and fault models, we can obtain a practical performance assessment of the algorithm for accurately and efficiently simulating the real implementation of quantum algorithms on NISQ devices.

**Baselines:** For evaluating the performance of our approximation algorithm, the baselines include the state-of-the-art accurate and approximate methods for simulating (noisy) quantum circuits.

The accurate methods include three types of noisy simulation algorithms, based on different data structures:

- *MM-based method: matrix multiplication-based method* has been widely used in the field of quantum simulation. In this case, input quantum states, gates and noises in simulated circuits are all treated as matrices, and the simulation is executed by matrix multiplications.
- *TDD-based method: tensor decision diagram-based method* uses decision diagrams style method for representing quantum states, gates and noises as tensors [32]. Subsequently, it is more efficient in equivalence checking of quantum circuits [33].
- *TN-based method: tensor network-based method* uses tensors to represent quantum states, gates and noises such that quantum circuits can be converted into a network of tensors. Then the noisy simulation is finished by contracting tensors in the network. The efficiency is highly dependent on the contraction order. In the following experiment, it is shown that the TN-based method is more efficient than the MM-based and TDD-based methods.

All the above methods will provide accurate simulation for noisy quantum circuits.

The approximate method is the quantum trajectories method [1]. It relies on a Monte Carlo approach, sampling the Kraus operators of a quantum noise based on probabilities. Consequently, it is a stochastic method and achieves a given accuracy probabilistically, while our approximation method is deterministic.

**Comparable Experiments:** We evaluate the efficiency of the aforementioned methods and our approximate techniques on benchmark circuits with realistic noises. The memory out (MO) limit is capped at 2048 GB.

*Our Algorithm vs. Accurate Methods:* First, we compare the three accurate methods on benchmark circuits with the number of noise being 2, and  $|\psi\rangle$  and  $|v\rangle$  are all chosen to be  $|0\rangle \otimes \dots \otimes |0\rangle$ . The result is shown in the columns of #Noise = 2 in Table II, where the timeout (TO<sub>1</sub>) thresholds are set at 3,600 seconds. As we can see from the table, the TN-based method outperforms the other methods, including our approximation algorithm in all three benchmarks. Thus, the TN-based method works very well for simulating noisy quantum circuits, so there is no need to apply our approximation algorithm. For complicated quantum circuits with a

larger number of noise, the TN-based method may fail, but our approximation algorithm works well.

To see this, we reset the noise number to 20, then we get the result in the columns of #Noise = 20 in Table II, where the timeout (TO<sub>2</sub>) threshold is set to be 36,000 seconds. From the result, *our approximation algorithm is more efficient than the TN-based method in the complex quantum circuits (with a larger number of qubits and depths)*, for example, see the rows of *qaoa\_121*, *qaoa\_225*, *inst\_4 × 5\_80* and *inst\_6 × 6\_20*.

Furthermore, to see the high efficiency of our approximation algorithm on the number of noises, we simulate the *qaoa\_100* circuit with 0 to 80 noises as shown in Fig. 4. Our approximation algorithm can handle all the cases, while the TN-based method runs out of memory after the noise number reaches 30. The main reason for memory exceed is that more noise may increase the nodes' maximum rank in the tensor network contraction and consume much time and memory for contraction. As a comparison, when using level-1 approximation of Algorithm 1, the runtime of our approximation algorithm is almost linear with the noise number as shown in Fig. 4.

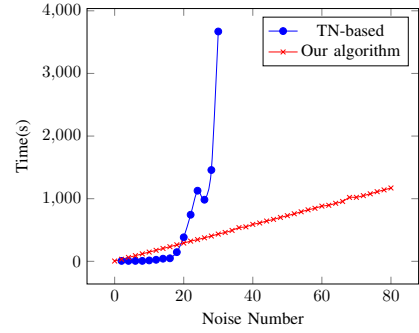


Fig. 4: The Number of Noises and Runtime.

*Our Algorithm vs. Approximate Methods:* Compared to the quantum trajectories method, we fixed the success probability for it at 99%. We then assessed the sample numbers for our algorithm and the quantum trajectories method at different noise rates  $p$ . For noise rates  $p = 0.001$  and  $p = 0.0001$ , and noise number  $n$  from 10 to 40, our method outperforms quantum trajectories for  $n \leq 26$  at  $p = 0.001$  and consistently at  $p = 0.0001$  (See Fig. 5).

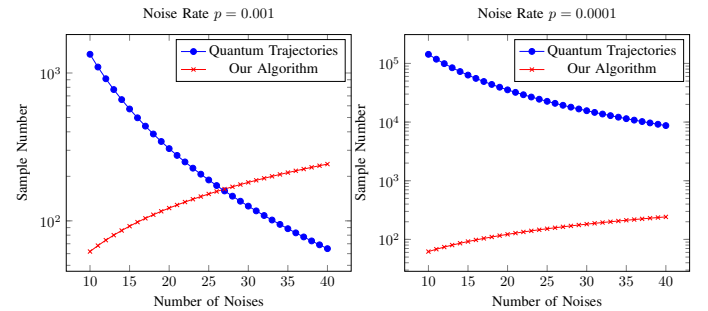


Fig. 5: Comparison of Sample Number Required for the Same Error Bound

TABLE II: OUR ALGORITHM VS. ACCURATE METHODS

Type	Circuit	Qubits	Gates	Depth	Time(s)					
					#Noise = 2			#Noise = 20		
					MM	TDD	TN	Ours	TN	Ours
HF-VQE	hf_6	6	155	72	0.17	1.2	0.095	0.81	0.093	15.74
	hf_8	8	308	124	0.24	3.65	0.33	1.52	0.31	28.63
	hf_10	10	461	142	26.91	7.59	0.37	2.81	0.39	40.11
	hf_12	12	690	194	206.37	18.81	0.99	3.56	0.98	64.28
QAOA	qaoa_64	64	1696	42	MO	58.33	3.51	15.96	47.38	182.32
	qaoa_121	121	3322	42	MO	225.76	9.77	49.96	1131.61	408.05
	qaoa_225	225	6330	42	MO	MO	925.87	2052.45	MO	6403.95
Supremacy	inst_4x4_10	16	115	11	MO	0.88	0.07	0.75	0.08	12.41
	inst_4x4_40	16	394	41	MO	TO <sub>1</sub>	4.34	26.04	MO	63.42
	inst_4x4_80	16	764	81	MO	TO <sub>1</sub>	11.26	39.69	MO	145.44
	inst_4x5_10	20	145	11	MO	1.52	0.10	1.42	0.1	11.30
	inst_4x5_20	20	261	21	MO	TO <sub>1</sub>	0.30	2.84	3725.2	21.09
	inst_4x5_80	20	959	81	MO	TO <sub>1</sub>	TO <sub>1</sub>	TO <sub>1</sub>	MO	26936
	inst_6x6_10	36	264	11	MO	0.77	0.22	5.71	0.26	356.82
	inst_6x6_20	36	483	21	MO	21.41	4.85	103.80	MO	428.74
inst_7x7_10	49	364	11	MO	1.66	0.45	2.22	0.75	21.95	

Furthermore, we conducted numerical experiments comparing our method’s efficiency and precision with various implementations of the quantum trajectories method, which is shown in Table. III. The quantum trajectories method was implemented in two ways: using MM-based [1] and TN-based simulator, respectively. Both tests used a depolarizing noise model with noise number 20 and rate  $p = 0.001$ . We adjusted the sample number for quantum trajectories to match the precision of our level-1 approximation. Seeing from Table. III, our method is more efficient than the quantum trajectories method at comparable precision levels (where "Traj" abbreviates the quantum trajectories method).

TABLE III: OUR ALGORITHM V.S. APPROXIMATE METHODS

Circuit	Precision			Runtime		
	Ours	Traj (MM)	Traj (TN)	Ours	Traj (MM)	Traj (TN)
QAOA_6	1.55E-04	1.43E-04	1.80E-04	4.56	1.49	10.84
QAOA_10	5.96E-05	1.98E-04	2.00E-04	7.57	10.94	19.68
QAOA_15	9.03E-05	2.55E-04	2.66E-04	8.41	658.38	25.48
QAOA_64	5.82E-07	MO	3.48E-07	191.47	MO	598.62
QAOA_100	1.03E-07	MO	1.30E-07	361.79	MO	1264.67

**Analytical Experiments:** We analyze our approximation algorithm in terms of noise rate and approximation levels.

(1) **Noise Rate:** The accuracy of our approximation algorithm depends on the noise rate of the noises, i.e.,  $p = \|M_{\mathcal{E}_D} - I\|$ . When  $p$  is small, the algorithm has a high accuracy. We evaluated our algorithm under both the realistic fault model and the depolarizing noise model. In both cases, the results as shown in Fig. 6 demonstrate that as the noise rate increases, the approximation error also rises. It confirms that our approximation algorithm has better accuracy for lower noise rates in realistic noise models, which indicates a promising outlook for achieving higher precision on advanced hardware implementations in the future.

(2) **Approximation Levels:** Our algorithm offers varying levels of approximation, presenting a trade-off between computational efficiency and accuracy. As a demonstration, we simulate *qaoa\_64* circuit with 10 noises. The input state  $|\psi\rangle = |0\rangle \otimes \dots \otimes |0\rangle$  and  $|v\rangle = U|0\rangle \otimes \dots \otimes |0\rangle$ , where  $U$

TABLE IV: ACCURACY FOR DIFFERENT APPROXIMATION LEVELS

Level	Time (s)	Result	Error
0	0.34	0.9539958	4.59E-03
1	11.18	0.9585521	3.02E-05
2	109.95	0.9585811	1.23E-06
3	1971.37	0.9585834	1.13E-06

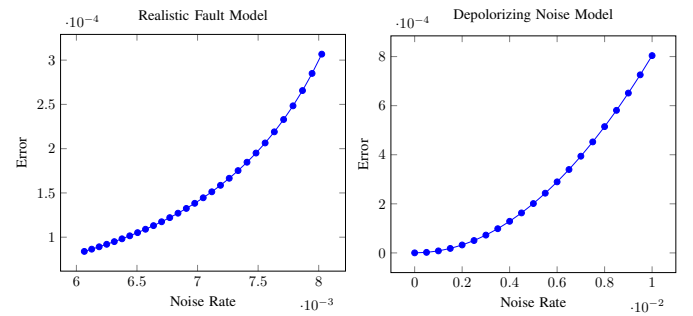


Fig. 6: Approximation error for different noise rate

represents the unitary operator of the ideal circuit. Table. IV shows the result for *qaoa\_64* circuit with approximation levels from 0 to 3. From the result, we can see that the accuracy is getting higher as expected, but the cost for an extra level of approximation is also significant. For most scenarios, the level-1 approximation is recommended since it can achieve a good balance between runtime and accuracy.

## VI. CONCLUSION

This paper presented a novel approximation algorithm for the noisy quantum circuit simulation task. Specifically, we introduced a new tensor network diagram for noisy quantum circuits and employed SVD to approximate the tensors representing quantum noises. In particular, our algorithm offers a speedup over the quantum trajectories method under the same approximation accuracy. Our algorithm is implemented with the Google TensorNetwork for contracting the tensor networks. The utility and effectiveness of our algorithm are



demonstrated by executing noisy simulations on three types of benchmark circuits with realistic noise models. The experimental results show that our approximation algorithm can simulate the 225-qubit QAOA circuit with 20 noises. Due to the scalability of qubits, we anticipate that our algorithm can serve as an integrated feature in the currently developed ATPG programs (e.g., [34]–[36]) for verifying and detecting manufacturing defects, effected by quantum noises, of large-size quantum circuits.

#### ACKNOWLEDGMENTS

This work was partly supported by the Youth Innovation Promotion Association, Chinese Academy of Sciences (No. 2023116), the National Natural Science Foundation of China (Grant No. 61832015).

#### REFERENCES

- [1] S. V. Isakov *et al.*, “Simulations of quantum circuits with approximate noise using qsim and cirq,” *arXiv preprint arXiv:2111.02396*, 2021.
- [2] F. Arute *et al.*, “Quantum supremacy using a programmable superconducting processor,” *Nature*, vol. 574, no. 7779, pp. 505–510, 2019.
- [3] M. Gong *et al.*, “Quantum walks on a programmable two-dimensional 62-qubit superconducting processor,” *Science*, vol. 372, no. 6545, pp. 948–952, 2021.
- [4] IBM. “Ibm unveils 400 qubit-plus quantum processor and next generation ibm quantum system two.” Accessed: 2023-05-22. (2022), [Online]. Available: <https://newsroom.ibm.com/2022-11-09-IBM-Unveils-400-Qubit-Plus-Quantum-Processor-and-Next-Generation-IBM-Quantum-System-Two>, 2022, ISSN: 1084-4309.
- [5] J. Preskill, “Quantum computing in the NISQ era and beyond,” *Quantum*, vol. 2, p. 79, 2018.
- [6] M. Harrigan *et al.*, “Quantum approximate optimization of non-planar graph problems on a planar superconducting processor,” *Nature Physics*, 2021.
- [7] Google AI Quantum and Collaborators *et al.*, “Hartree-fock on a superconducting qubit quantum computer,” *Science*, vol. 369, no. 6507, pp. 1084–1089, 2020.
- [8] S. Boixo *et al.*, “Characterizing quantum supremacy in near-term devices,” *Nature Physics*, vol. 14, pp. 595–600, 2018.
- [9] T. Häner and D. S. Steiger, “5 petabyte simulation of a 45-qubit quantum circuit,” in *Proceedings of the International Conference for High Performance Computing, Networking, Storage and Analysis*, 2017, pp. 1–10.
- [10] C. Huang *et al.*, “Classical simulation of quantum supremacy circuits,” *arXiv preprint arXiv:2005.06787*, 2020.
- [11] R. Li, B. Wu, M. Ying, X. Sun, and G. Yang, “Quantum supremacy circuit simulation on sunway taihulight,” *IEEE Transactions on Parallel and Distributed Systems*, vol. 31, no. 4, pp. 805–816, 2019.
- [12] E. Pednault *et al.*, “Breaking the 49-qubit barrier in the simulation of quantum circuits,” *arXiv preprint arXiv:1710.05867*, vol. 15, 2017.
- [13] B. Villalonga *et al.*, “A flexible high-performance simulator for verifying and benchmarking quantum circuits implemented on real hardware,” *npj Quantum Information*, vol. 5, no. 1, pp. 1–16, 2019.
- [14] F. Pan and P. Zhang, “Simulation of quantum circuits using the big-batch tensor network method,” *Phys. Rev. Lett.*, vol. 128, p. 030 501, 3 Jan. 2022.
- [15] Y.-H. Tsai, J.-H. R. Jiang, and C.-S. Jhang, “Bit-slicing the hilbert space: Scaling up accurate quantum circuit simulation,” in *2021 58th ACM/IEEE Design Automation Conference (DAC)*, San Francisco, CA, USA: IEEE Press, 2021, pp. 439–444.
- [16] A. Zulehner and R. Wille, “Advanced simulation of quantum computations,” *IEEE Transactions on Computer-Aided Design of Integrated Circuits and Systems*, vol. 38, no. 5, pp. 848–859, 2018.
- [17] S. Hillmich, R. Kueng, I. L. Markov, and R. Wille, “As accurate as needed, as efficient as possible: Approximations in dd-based quantum circuit simulation,” in *2021 Design, Automation & Test in Europe Conference & Exhibition (DATE)*, IEEE, 2021, pp. 188–193.
- [18] Qiskit contributors, *Qiskit: An open-source framework for quantum computing*, 2023.
- [19] C. Developers, *Cirq*, version v1.1.0. See full list of authors on Github: <https://github.com/quantumlib/Cirq/graphs/contributors>, Dec. 2022.
- [20] Y. Zhou, E. M. Stoudenmire, and X. Waintal, “What limits the simulation of quantum computers?” *Physical Review X*, vol. 10, no. 4, p. 041 038, 2020.
- [21] K. Woolfe, “Matrix product operator simulations of quantum algorithms,” Ph.D. dissertation, University of Melbourne, School of Physics, 2015.
- [22] K. Noh, L. Jiang, and B. Fefferman, “Efficient classical simulation of noisy random quantum circuits in one dimension,” *Quantum*, vol. 4, p. 318, 2020.
- [23] S. Cheng *et al.*, “Simulating noisy quantum circuits with matrix product density operators,” *Physical Review Research*, vol. 3, no. 2, p. 023 005, 2021.
- [24] T. Grull, J. Fuß, and R. Wille, “Noise-aware quantum circuit simulation with decision diagrams,” *IEEE Transactions on Computer-Aided Design of Integrated Circuits and Systems*, pp. 1–1, 2022.
- [25] C. Roberts *et al.*, *Tensornetwork: A library for physics and machine learning*, 2019.
- [26] M. A. Nielsen and I. L. Chuang, *Quantum computation and quantum information*. Cambridge university press, 2010.
- [27] J. Biamonte and V. Bergholm, “Tensor networks in a nutshell,” *arXiv preprint arXiv:1708.00006*, 2017.
- [28] J. Watrous, *The theory of quantum information*. Cambridge university press, 2018.
- [29] C. Eckart and G. Young, “The approximation of one matrix by another of lower rank,” *Psychometrika*, vol. 1, no. 3, pp. 211–218, 1936.
- [30] Quantum AI team and collaborators, *Recirq*, Oct. 2020.
- [31] Q. Huang, B. Li, M. Gao, and M. Ying, *Fault models in superconducting quantum circuits*, 2022.
- [32] X. Hong, X. Zhou, S. Li, Y. Feng, and M. Ying, “A tensor network based decision diagram for representation of quantum circuits,” *ACM Transactions on Computer-Aided Design of Integrated Circuits and Systems*, vol. 37, no. 3, pp. 587–600, 2017.
- [33] X. Hong, M. Ying, Y. Feng, X. Zhou, and S. Li, “Approximate equivalence checking of noisy quantum circuits,” in *2021 58th ACM/IEEE Design Automation Conference (DAC)*, 2021, pp. 637–642.
- [34] X. Fang-ying, C. Han-wu, L. Wen-jie, and L. Zhi-giang, “Fault detection for single and multiple missing-gate faults in reversible circuits,” in *2008 IEEE Congress on Evolutionary Computation (IEEE World Congress on Computational Intelligence)*, IEEE, 2008, pp. 131–135.
- [35] A. Paler, I. Polian, and J. P. Hayes, “Detection and diagnosis of faulty quantum circuits,” in *17th Asia and South Pacific Design Automation Conference*, IEEE, 2012, pp. 181–186.
- [36] D. Bera, “Detection and diagnosis of single faults in quantum circuits,” *IEEE Transactions on Computer-Aided Design of Integrated Circuits and Systems*, vol. 37, no. 3, pp. 587–600, 2017.